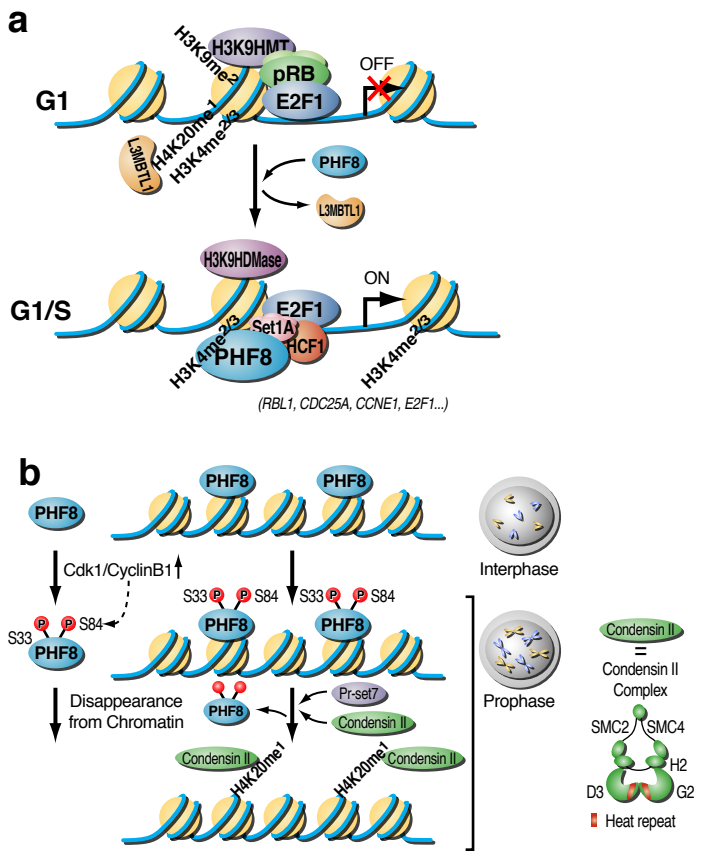

Figure S1. PHF8 mediated histone H4 lysine 20 demethylation events involved in cell cycle progression. a, Model of regulation of cell cycle genes in G1-S transition by PHF8 based on its H4K20me^1 demethylase activity. **b,** Model of regulation of mitosis by PHF8, with phospho-PHF8 dissociation from chromatin in early mitosis linking accumulation of H4K20me^1 with Condensin II complex recruitment.

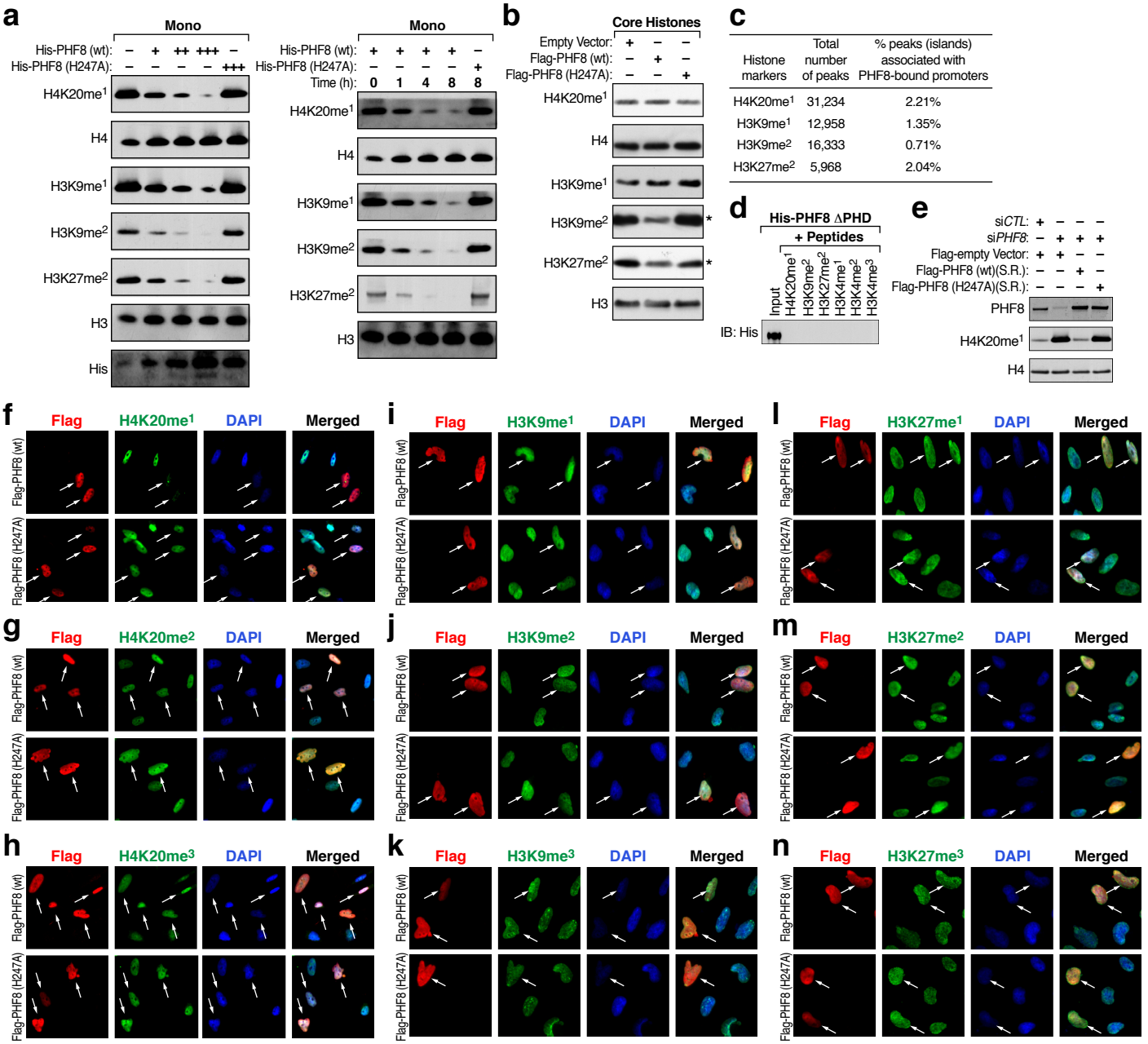

Figure S2. PHF8 demethylase activity. a, PHF8 demethylase activity assessed in both dose-dependent (left panels) and time-course experiments (right panels). Left panels: His-tagged full length wild-type (with increasing amount) or mutant PHF8 proteins were incubated with mononucleosomes for 4 hrs, analyzed by immunoblotting as indicated (-, +, ++ and +++ represent 0, 2.5, 5 and 10 μg protein, respectively). Right panels: 5 μg of His-tagged full-length wild-type or mutant PHF8 proteins were incubated with mononucleosomes for various time periods, analyzed by immunoblotting as indicated. **b,** Demethylase activity of Flag-tagged full-length wild-type and mutant (H247A) PHF8 immunoprecipitated from HEK293T cell lysates was assessed using core histones as substrates. Asterisk denotes potential substrate. **c,** ChIP-Seq analysis and peak (island) finding for histone marks as indicated and percentage of these peaks associated with PHF8 promoter peaks. **d,** Peptide pull-down assay mixing purified bacterially-expressed His-tagged delta PHD PHF8 (aa 55-1024) with various biotinylated histone tails as indicated. Pull-downs were analyzed by immunoblotting. **e,** HeLa cells were transfected with control or *PHF8* siRNA and empty vector, wild-type or mutant (H247A) PHF8 with non-sense mutations at siRNA targeting sequence, and analyzed by immunoblotting as indicated. (S.R.=siRNA resistant) **f-n,** Immunohistochemical analysis of HeLa cells transfected with Flag-tagged wild-type or mutant (H247A) PHF8. Cells were stained with anti-flag (red) and anti-H4K20me^1 (f), anti-H4K20me^2 (g), anti-H4K20me^3 (h), anti-H3K9me^1 (i), anti-H3K9me^2 (j), anti-H3K9me^3 (k), anti-H3K27me^1 (l), anti-H3K27me^2 (m) or anti-H3K27me^3 (n) (green). Nuclei were counterstained with DAPI (blue). White arrows indicate cells transfected with PHF8.

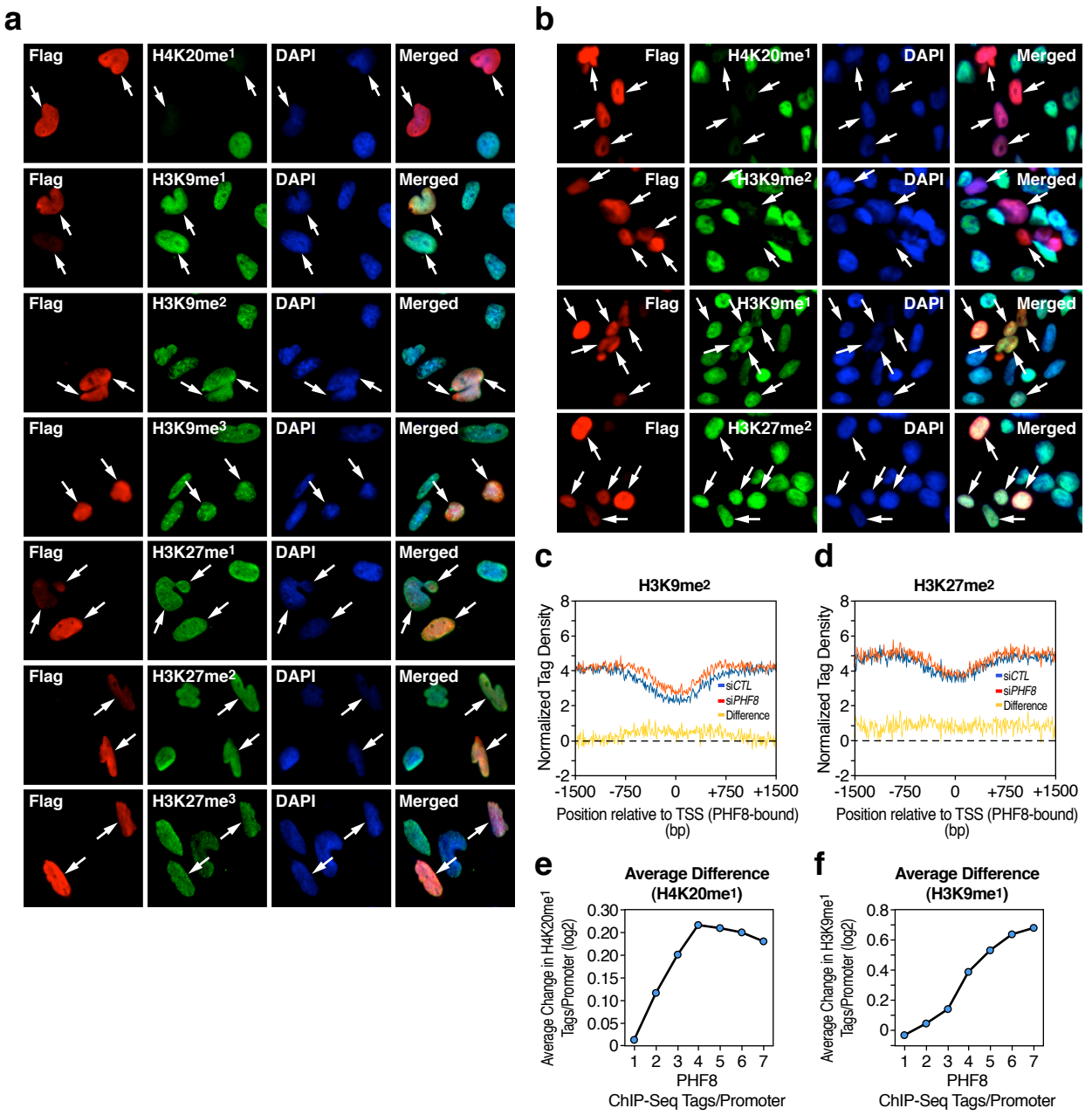

Figure S3. PHF8 demethylase activity. a, Immunohistochemical analysis of HeLa cells transfected with Flag-tagged PHF8 (1-447) fused with a nuclear localization signal. Cells were stained with anti-flag (red) and anti-H4K20me^1, anti-H3K9me^1, anti-H3K9me^2, anti-H3K9me^3, anti-H3K27me^1, anti-H3K27me^2 or anti-H3K27me^3 (green), as indicated. Nuclei were counterstained with DAPI (blue). White arrows indicate PHF8 transfected cells. **b,** Immunohistochemical analysis of U2OS cells transfected with Flag-tagged PHF8. Cells were stained with anti-flag (red) and anti-H4K20me^1, anti-H3K9me^2, anti-H3K9me^1 or anti-H3K27me^2 (green), as indicated. Nuclei were counterstained with DAPI (blue). White arrows indicate cells transfected with PHF8. **c-d,** H3K9me^2 (c) or H3K27me^2 (d) ChIP-Seq tags distribution over PHF8 promoter regions in control and *PHF8* siRNA transfected HeLa cells. **e-f,** Graphs displaying the relationship between levels of PHF8 ChIP-Seq tags and the change in H4K20me^1 (e) or H3K9me^1 (f) levels on individual promoter for all promoters in the genome. Promoters were binned by the levels of PHF8 ChIP-Seq tags (within +/- 500 bp) from the TSS. Difference in H4K20me^1 (e) or H3K9me^1 (f) levels between *PHF8* and control siRNA were reported as an average for all promoters in the same bin. As shown, the difference in H4K20me^1 (e) or H3K9me^1 (f) levels between *PHF8* siRNA transfected cells and control cells correlated with PHF8 ChIP-Seq tags on all promoters in the genome (e.g., the less PHF8 tags a promoter has, the less change of H4K20me^1 or H3K9me^1 could be observed when depleting PHF8, and vice versa).

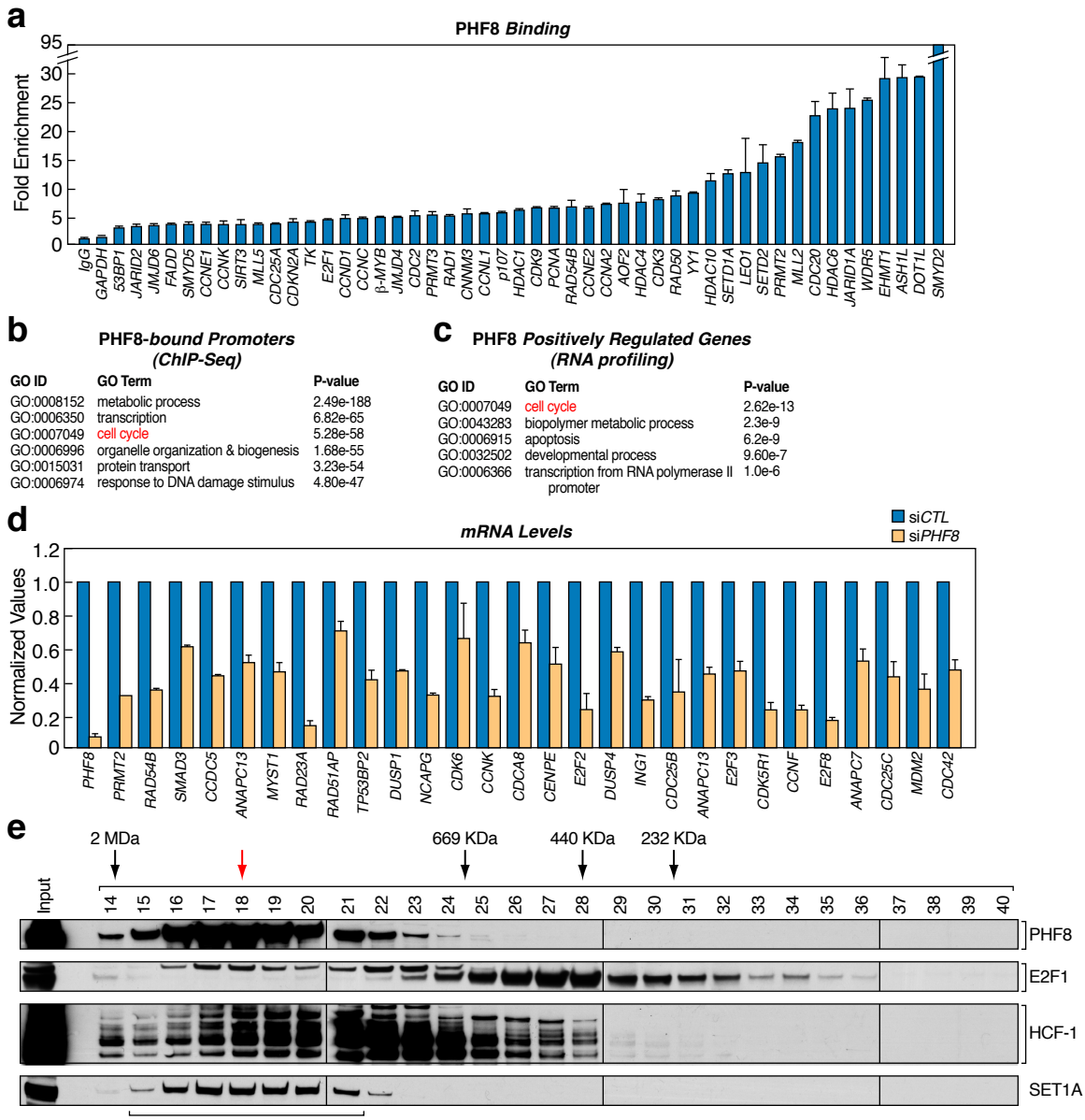

Figure S4, Characterization of PHF8 protein. a, Validation of PHF8 binding by ChIP-qPCR. HeLa cells were subjected to standard ChIP assay. ChIP signals for PHF8 were presented as fold enrichment over that of IgG (± s.e.m.). All the selected PHF8 binding sites identified by ChIP-Seq showed enrichment over IgG and a predicted negative control (*GAPDH* promoter region). **b,** Gene ontology analysis of PHF8 bound promoters (n=10,495) revealed by ChIP-Seq in HeLa cells. **c,** Gene ontology analysis of genes positively regulated by PHF8 revealed by RNA profiling using samples from HeLa cells transfected with control or *PHF8* siRNA. **d,** Validation of PHF8 positively regulated genes revealed by RNA profiling through RT-qPCR. RNA samples extracted from HeLa cells transfected with either control or *PHF8* siRNAs were subjected to RT-qCR analysis by using primers specific for the genes as indicated. Data shown is the relative fold change comparing *PHF8* siRNA to control siRNA transfected samples for each individual gene after normalized to actin (± s.e.m.). **e,** HeLa nuclear extracts were analyzed by size exclusion chromatography (Superose-6). Collected fractions were then subjected to western blotting analysis as indicated. From fractions 15 to 21, a peak of PHF8/E2F1/HCF-1/SET1A is seen at fraction 18, as indicated by red arrow. Molecular mass markers are shown on top.

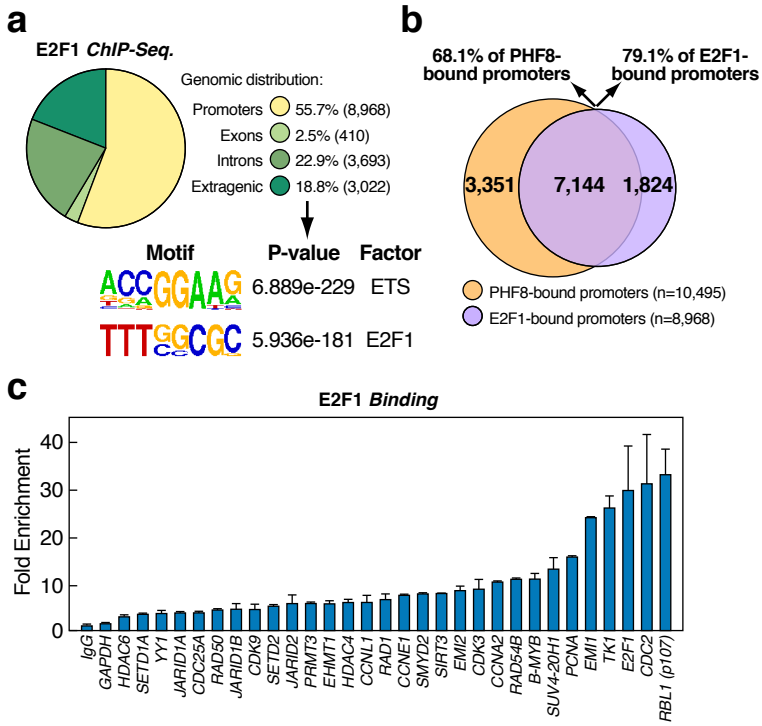

Figure S5, E2F1 ChIP-Seq and its association with PHF8. a, Genomic distribution and top enriched motifs of E2F1 ChIP-Seq peaks (n=16,093) in HeLa cells. **b,** Venn diagram showing overlap between PHF8 and E2F1-bound promoters (n=10,495 and 8,968, respectively). **c,** Validation of E2F1 binding by ChIP-qPCR as described in Fig. S4a. All the selected E2F1 binding sites identified by ChIP-Seq showed enrichment over IgG and a predicted negative control (GAPDH promoter region) (± s.e.m.).

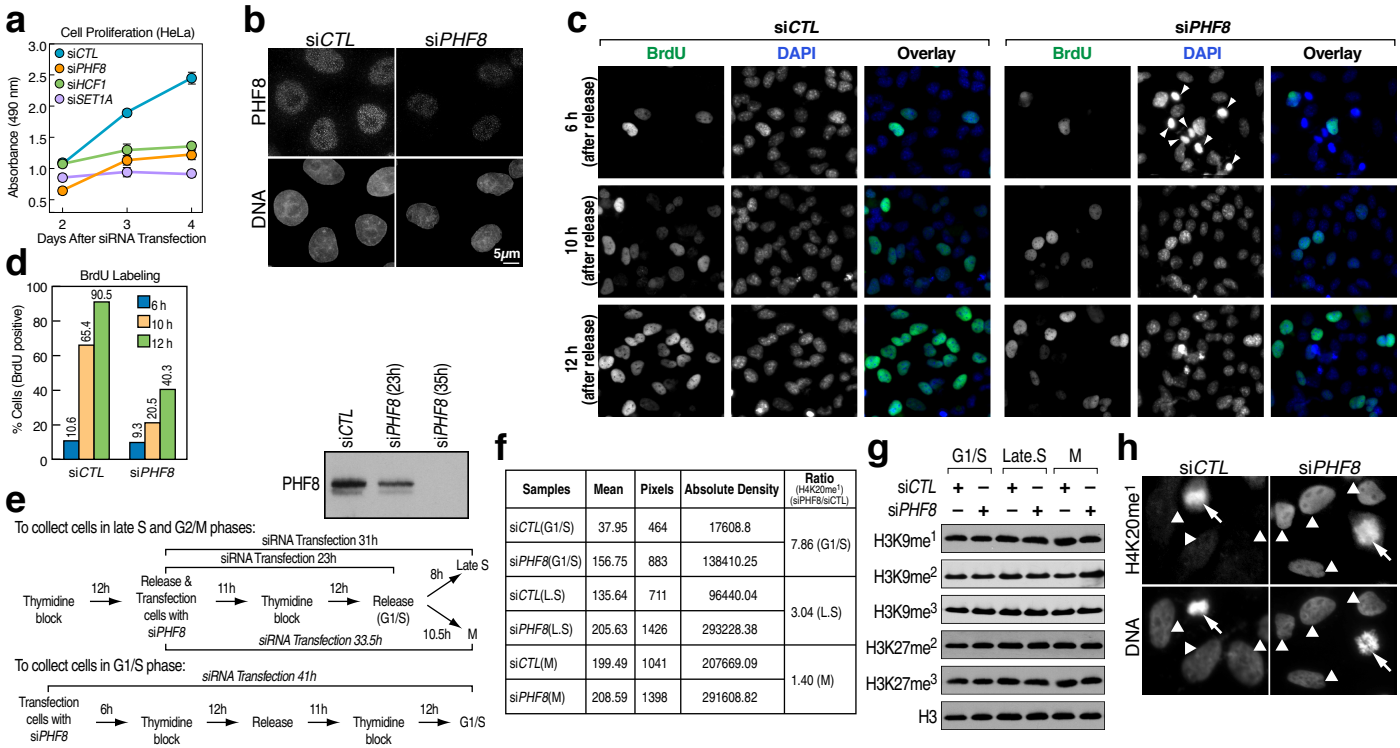

Samples	Mean	Pixels	Absolute Density	Ratio (H4K20me1) (siPHF8/siCTL)
si*CTL*(G1/S)	37.95	464	17608.8	7.86 (G1/S)
si*PHF8*(G1/S)	156.75	883	138410.25	
si*CTL*(L.S)	135.64	711	96440.04	3.04 (L.S)
si*PHF8*(L.S)	205.63	1426	293228.38	
si*CTL*(M)	199.49	1041	207669.09	1.40 (M)
si*PHF8*(M)	208.59	1398	291608.82	

Figure S6, PHF8 knock-down leads to G1-S transition delay in HeLa cells. a, Cell viability analysis of HeLa cells transfected with control, *PHF8, HCF-1* or *SET1A* siRNA at various time points as indicated. **b,** HeLa cells were transfected with control or *PHF8* siRNAs, immunostained with anti-PHF8 (top panel) or DAPI (bottom panel). Scale bar, 5 μm. **c,** Kinetics of BrdU incorporation in HeLa cells transfected with either control or *PHF8* siRNAs and released from a mitotic arrest. S phase entry was measured by determining BrdU incorporation at 6, 10 and 12 h, presumably, cells are in late G1, early S and mid S phases, respectively. Cells were stained with BrdU (green) and DAPI (Blue) as indicated. Arrowheads denote mitotic cells with condensed chromosomes. **d,** Bar graph displaying percentage of BrdU positive stained cells in HeLa cell transfected with control or *PHF8* siRNAs and released from a mitotic arrest as described in (c) (n=500). **e,** Modified synchronization protocol followed to collect cells in S, G2-M or G1-S with control or *PHF8* siRNA transfection, which allowed cells to escape the G1-S border since PHF8 was still not significantly depleted after 23 h siRNA transfection, but 8 h or 10.5 h after releasing from the second thymidine treatment, cells presumably entered into late S or M phase, respectively, with a significant depletion of PHF8 protein, as shown by immunoblotting. **f,** Ratios of H4K20me^1 between *PHF8* and control siRNA samples in G1-S, S and M phases as described in Fig. 2g. Densitometry was carried out in Photoshop. **g,** Chromatin-bound fractions from HeLa cells transfected with control or *PHF8* siRNAs and synchronized to different cell cycle phases as indicated were analyzed by immunoblotting. **h,** HeLa cells were transfected with control or *PHF8* siRNAs, immunostained with H4K20me^1 (top panel) and DAPI (bottom panel). Interphase and mitotic cells are indicated by arrowheads and arrows, respectively. A significant increase of H4K20me^1 was observed in interphase cells, but not in mitotic cells.

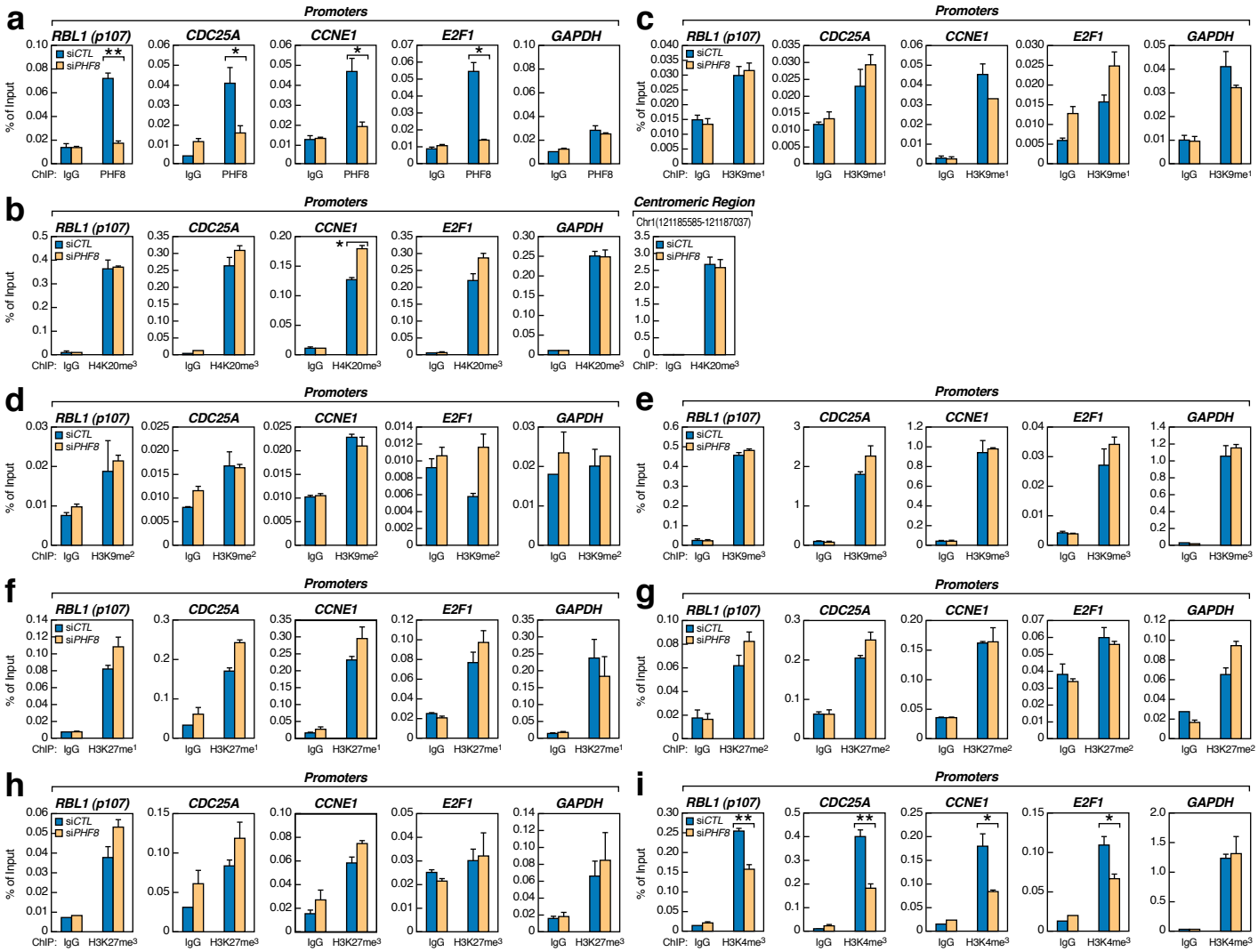

Figure S7, Changes in PHF8, H4K20me^3, H3K9me$^{1/2/3}$, H3K27me$^{1/2/3}$ and H3K4me^3 occupancy on *RBL1(p107), CDC25A, CCNE1, E2F1* and *GAPDH* promoter regions upon PHF8 knock-down. ChIP analysis of PHF8 (a) or histone marks, including H4K20me^3 (b), H3K9me^1 (c), H3K9me^2 (d), H3K9me^3 (e), H3K27me^1 (f), H3K27me^2 (g), H3K27me^3 (h) and H3K4me^3 (i) on selected cell cycle-regulated gene as well as *GAPDH* promoter region in HeLa cells transfected with control or *PHF8* siRNAs as indicated. ChIP signals were presented as percentage of input (± s.e.m., *p<0.05, **p<0.01). ChIP for H4K20me^3 on centromeric region was shown as a positive control.

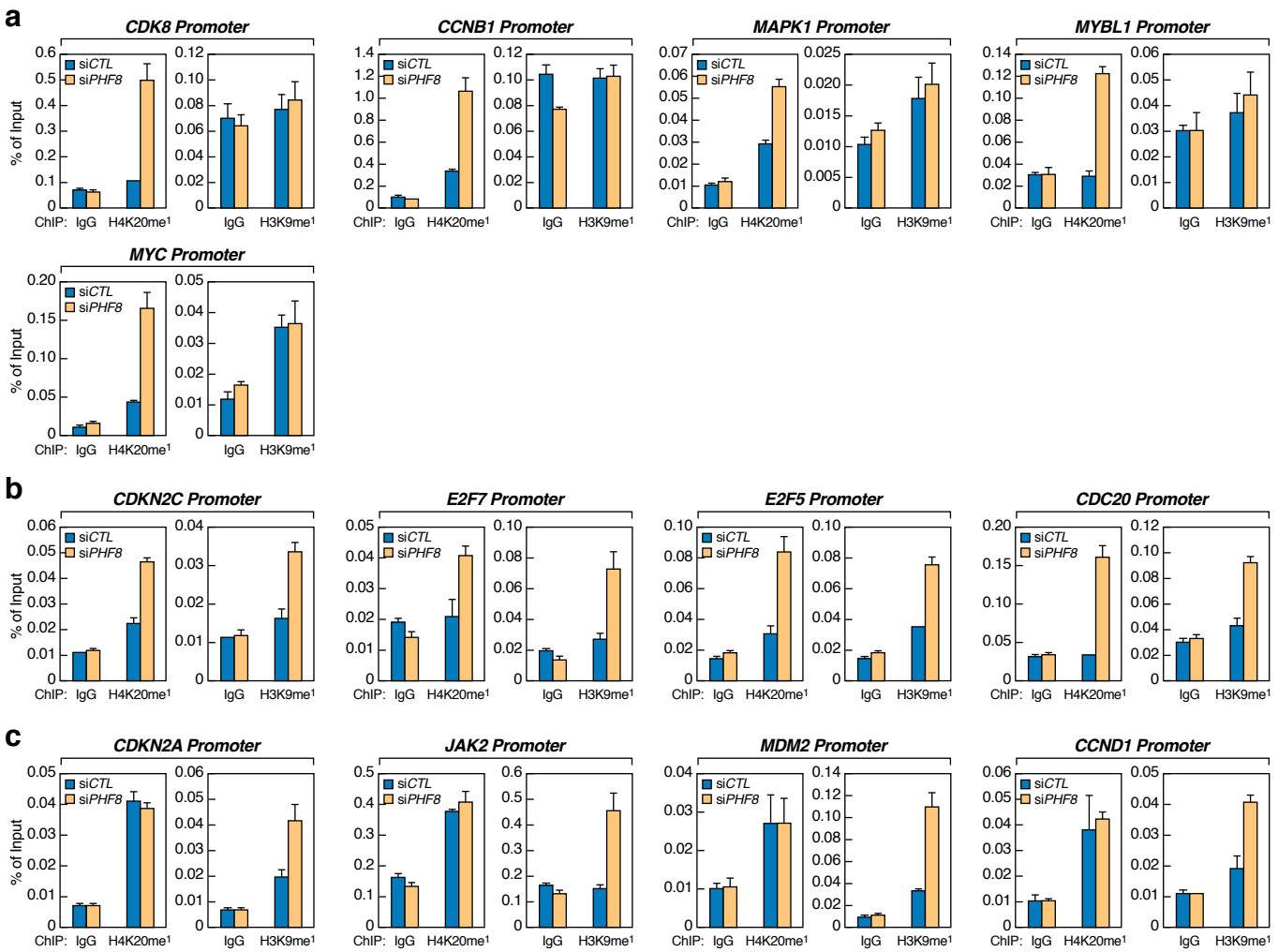

Figure S8, H4K20me^1 and H3K9me^1 occupancy on selected PHF8-bound promoter regions. ChIP analysis of histone marks, including H4K20me^1 and H3K9me^1 on selected PHF8-bound promoter regions in HeLa cells transfected with control or *PHF8* siRNAs as indicated. ChIP signals were presented as percentage of input (± s.e.m.). Representative promoters with only H4K20me^1 (a) or H3K9me^1 (c) change, or both H4K20me^1 and H3K9me^1 changes (b) were shown.

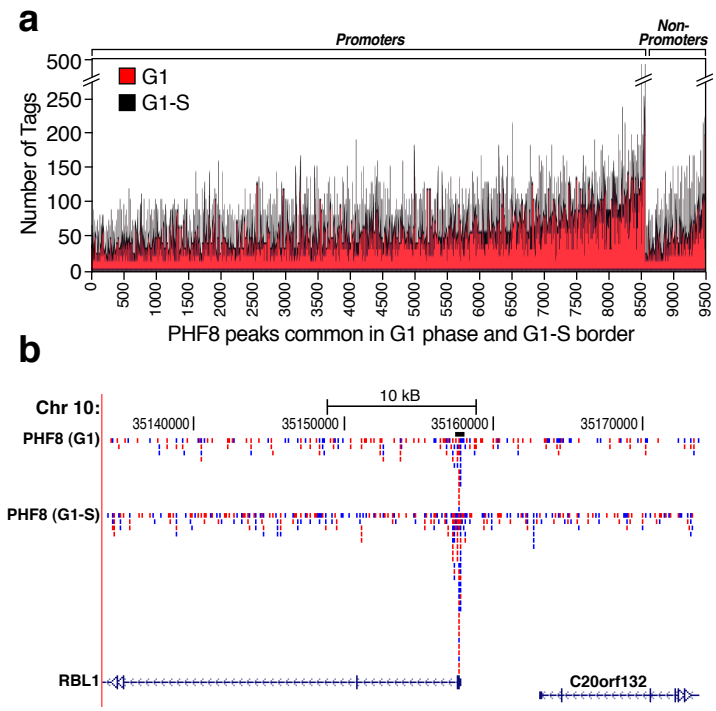

Figure S9, PHF8 ChIP-Seq in G1 phase and G1-S border. a, Tags distribution over PHF8 binding sites common in G1 phase and G1-S border revealed by ChIP-Seq. Both promoter and non-promoter regions were shown as indicated. **b,** PHF8 ChIP-Seq tags in G1 phase or G1-S border on promoter region of *RBL1(p107)* gene locus in HeLa cells.

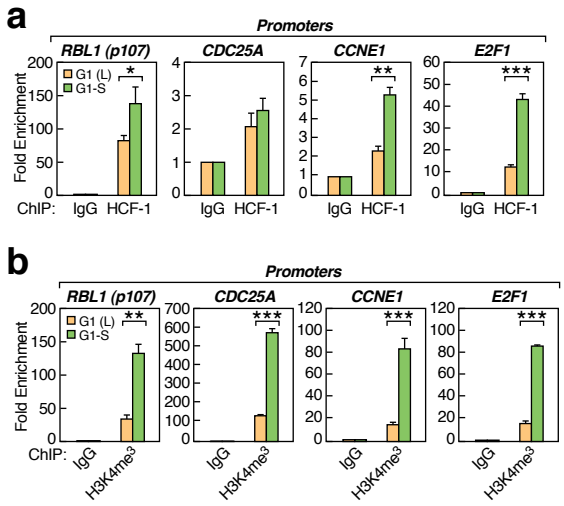

Figure S10, HCF-1 binding and H3K4me^3 occupancy during G1-S transition in cell cycle. ChIP analysis of HCF-1 (a) or H3K4me^3 (b) on selected cell cycle-regulated gene promoter regions in HeLa cells synchronized to G1 phase or G1-S border phases as indicated. (± s.e.m., **p<0.01, ***p<0.001).

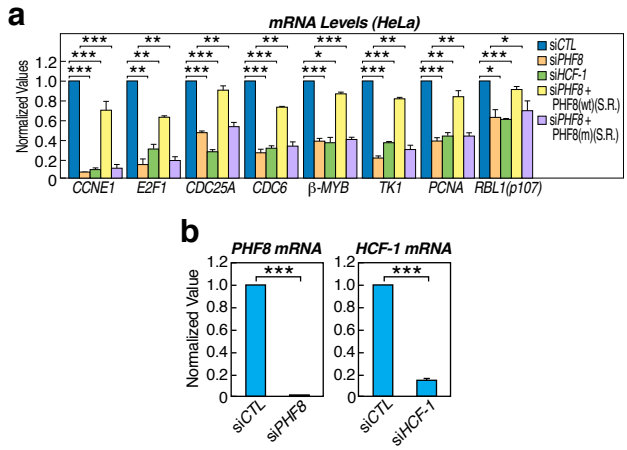

Figure S11, PHF8 and HCF-1 knock-down blocked induction of G1-S transition-regulated genes bound by both PHF8 and E2F1. **a,** mRNA levels of selected genes in HeLa cells transfected with control, *PHF8* or *HCF-1* siRNAs alone or with or without wild-type or mutant (H247A) PHF8 measured by RT-qPCR. (S.R.= siRNA resistance). **b.** mRNA levels of *PHF8* (left panel) and *HCF-1* (right panel) in HeLa cells transfected with either control, *PHF8* or *HCF-1* siRNAs, as described in (a), detected by RT- qPCR. Data shown is the relative fold change compared to control siRNA transfected samples after normalized to actin (± s.e.m., *p<0.05, **p<0.01, ***p<0.001).

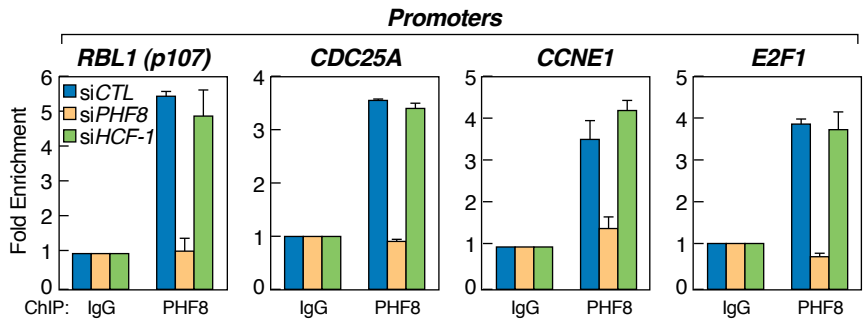

Figure S12, *HCF-1* knock-down has no effect on PHF8 binding. ChIP of PHF8 on selected cell cycle gene promoter regions in HeLa cells transfected with control, *PHF8* or *HCF-1* siRNAs as indicated. ChIP signals for PHF8 were presented as fold enrichment over IgG ChIP signals (± s.e.m.).

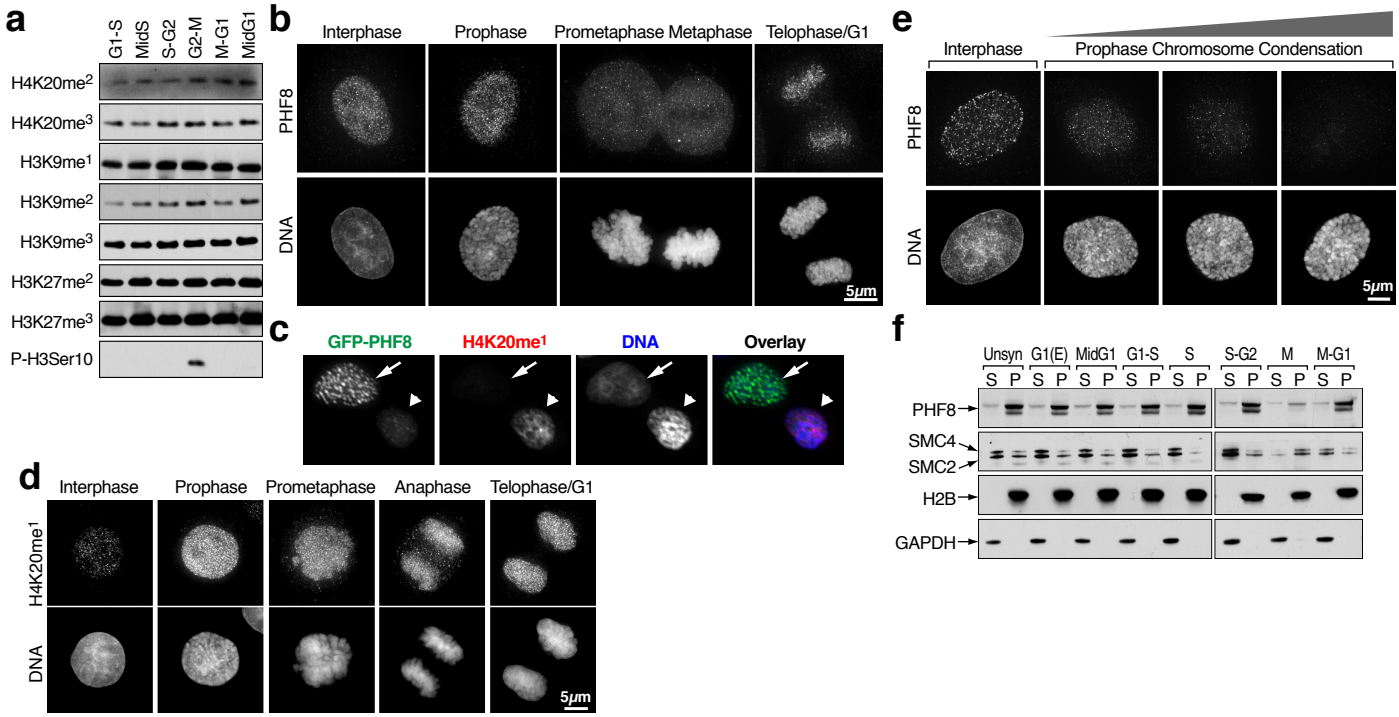

Figure S13, PHF8 dissociates from chromatin in prophase. a, Chromatin-bound fractions from HeLa cells synchronized to different cell cycle phases were analyzed by immunoblotting as indicated. **b,** Asynchronously growing HeLa cells were directly fixed and stained with PHF8. Nuclei (DNA) were stained with Hoechst dye. Representative images for different cell cycle phases were shown as indicated. Scale bar, 5 μm. **c,** HeLa cells transfected with GFP-tagged PHF8 were pre-extracted with 0.1% Triton X-100, fixed and stained with anti-H4K20me^1 (red). Nuclei were stained with DAPI. Arrow and arrowhead denote interphase and prophase cells, respectively. **d,** Asynchronously growing HeLa cells were pre-extracted with 0.1% Triton X-100, fixed and stained with H4K20me^1 as indicated. Nuclei (DNA) were stained with Hoechst dye. Representative images for different cell cycle phases were shown as indicated. Scale bar, 5 μm. **e,** PHF8 gradually dissociates from chromatin as cell condenses its chromosomes in prophase. Asynchronously growing HeLa cells were pre-extracted with 0.1% Triton X-100, fixed and stained with PHF8. Nuclei (DNA) were stained with Hoechst dye. Representative images for interphase and prophase cells were shown as indicated. Scale bar, 5 μm. **f,** Chromatin-free (S, soluble) and –bound (P, pellet) fractions were prepared from HeLa cells synchronized to different cell cycle phases and analyzed by immunoblotting as indicated.

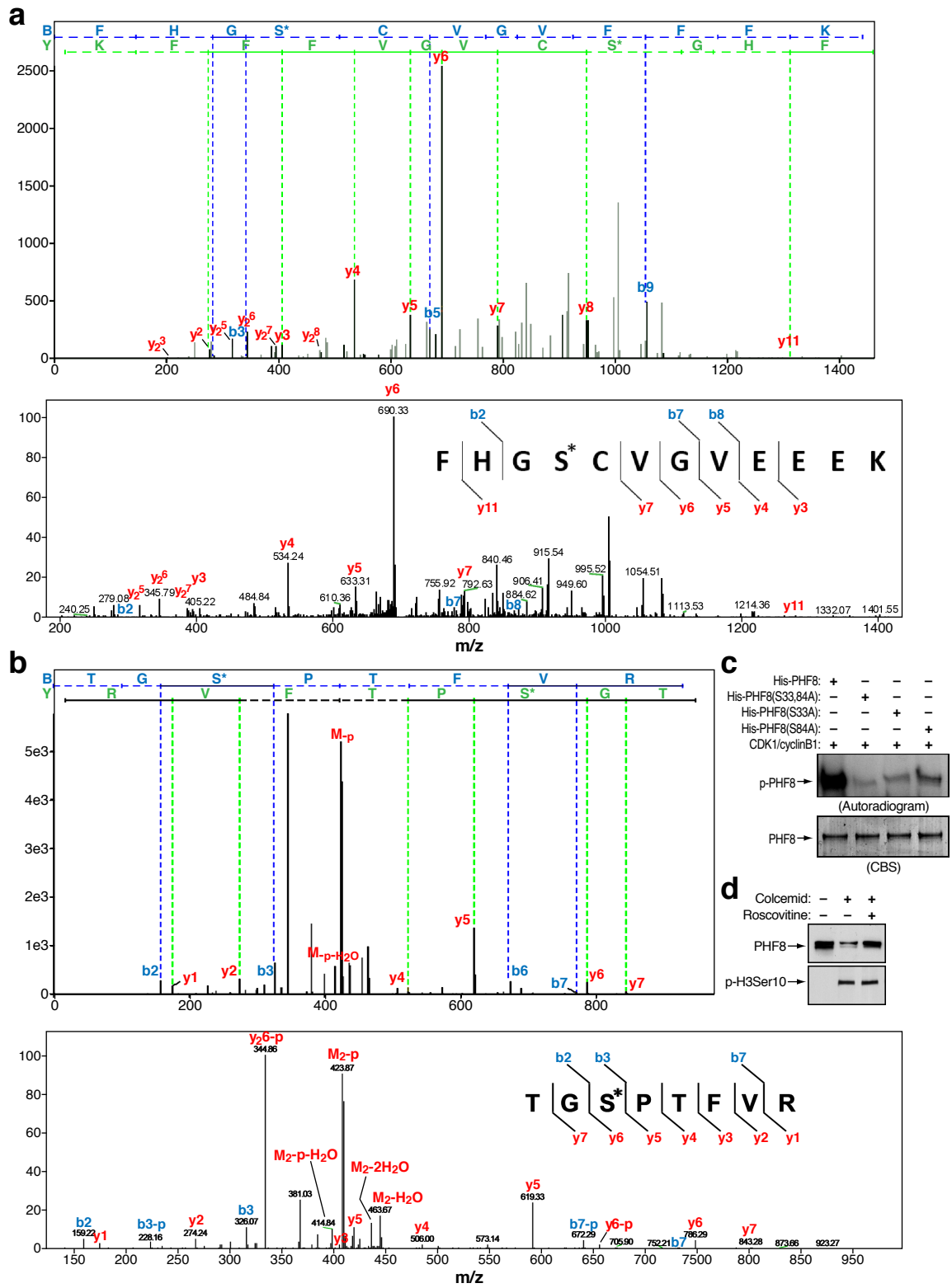

Figure S14, Tandem MS spectrum revealed two putative phosphorylation sites on PHF8 by CDK1/cyclinB1 at Serine 33 and 84. **a-b,** *In vitro* kinase assay was performed by mixing CDK1/cyclinB1 with purified bacterially-expressed PHF8 protein. The reaction mixture were then digested with Trypsin singles proteomic grade and subjected to Capillary-LC analysis. InsPecT was applied to search for phosphorylated peptides on a serine, threonine or tyrosine with a mass shift of 80 Da. The parent ion mass tolerance was set to be 2 Da and b, y ion mass tolerance was set as 0.5 Da. Tandem MS spectrum revealed two putative phosphorylation sites on PHF8 by CDK1/cyclinB1 at Serine33 (a) and Serine 84 (b). P represents H3PO4. **c,** *In vitro* phosphorylation of His-tagged wild-type and phosphorylation mutant PHF8 by CDK1/cyclinB1. Protein expression was visualized by commassie blue staining (bottom panel). **d,** HeLa cells were pre-treated with or without colcemid (1 μm) for 20 h before adding DMSO vehicle or Roscovitine (10 μm) and chromatin bound fractions were analyzed by immunoblotting as indicated.

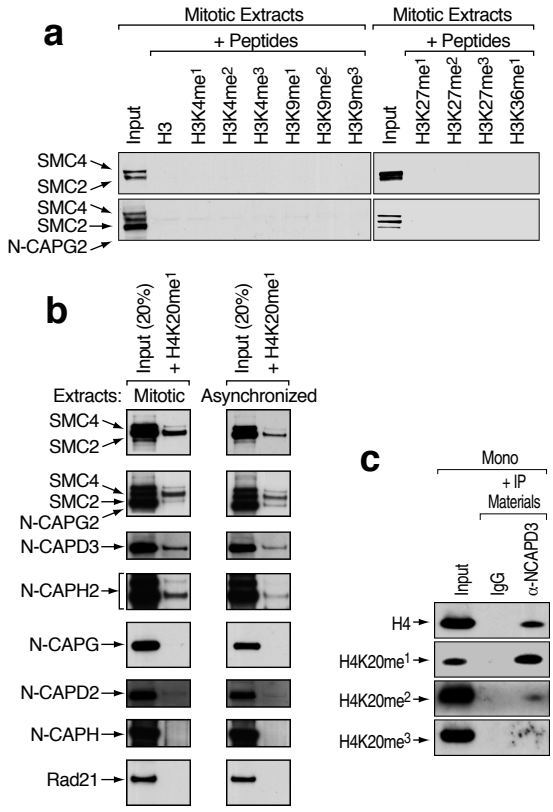

Figure S15, Specific interaction between Condensin II complex and H4K20me1 histone tails. a, Peptide pull-down assays were performed mixing HeLa mitotic extracts with biotinylated histone tails. Pull-downs were analyzed by immunoblotting as indicated. **b,** Peptide pull-down assay by mixing HeLa mitotic (left panels) or asynchronized (right panels) cell extracts with biotinylated H4K20me1 histone tails. Pull-downs were analyzed by immunoblotting with antibodies against individual subunits in both Condensin I and II complexes or Rad21, a component of the cohesin complex as indicated. **c,** Immunoprecipitates from a negative IgG control or a specific antibody against N-CAPD3 were mixed with mononucleosomes purified from HeLa cells. Pull-downs were analyzed by immunoblotting as indicated.

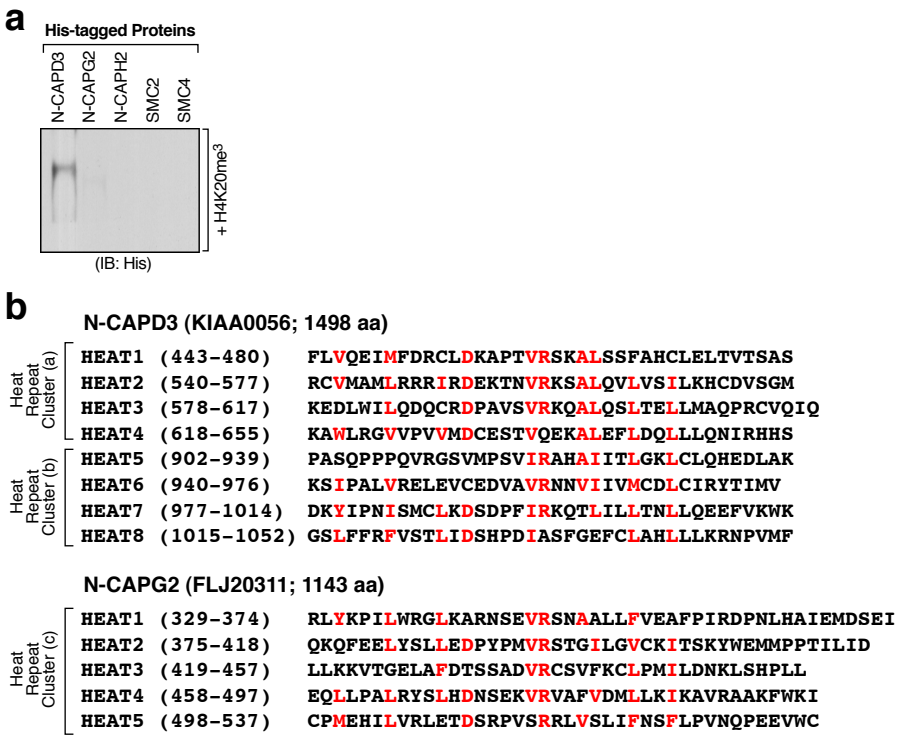

Figure S16, Heat repeat clusters in N-CAPD3 and N-CAPG2. a, Peptide pull-down assays were performed by mixing purified bacterially-expressed full length N-CAPD3, N-CAPG2, N-CAPH2, SMC2 or SMC4 with biotinylated H4K20me^3 histone tails. Pull-downs were analyzed by immunoblotting as indicated. **b,** HEAT repeats in N-CAPD3 and N-CAPG2. HEAT repeat cluster (a) in N-CAPD3 contains 4 continuous Heat repeats from aa 443-655; Heat repeat cluster (b) in N-CAPD3 contains 4 continuous HEAT repeats from aa 902-1052; HEAT repeat cluster (c) in N-CAPG2 contains 5 continuous HEAT repeats from aa 329-537. Consensus sequence in HEAT repeat was highlighted in red. Please also see reference (Ono, et al).

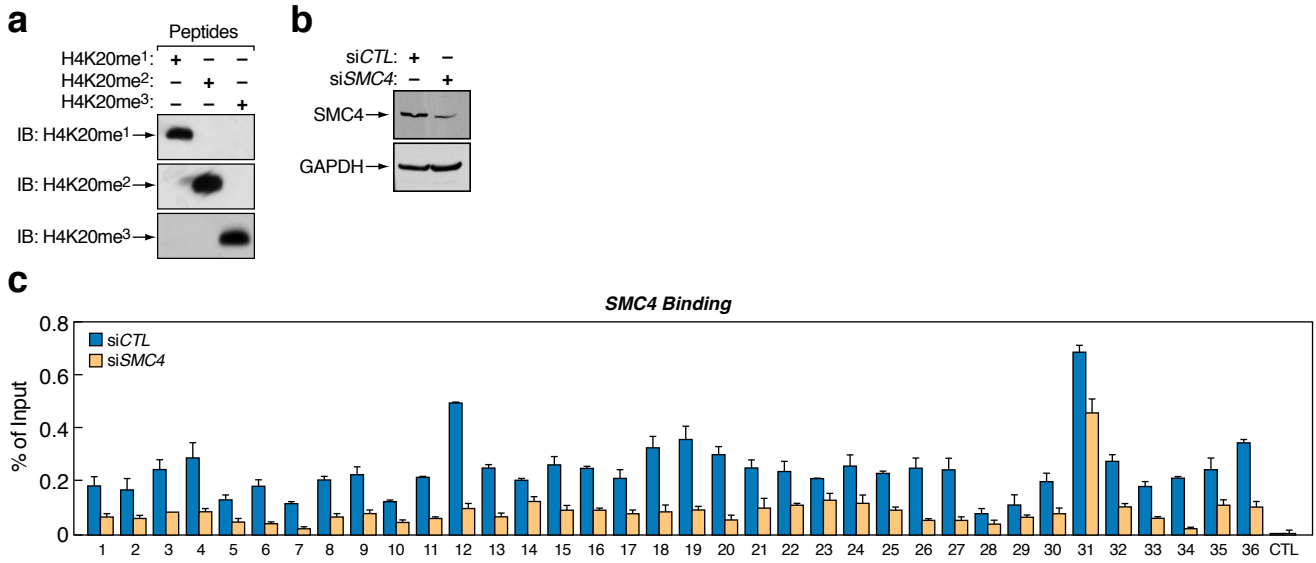

Figure S17, SMC4 and H4K20me1 ChIP-Seq in M phase HeLa cells. a, Specificity of the H4K20me$^{1/2/3}$ antibodies shown by immunoblotting with histone H4 tails mono-, di- or tri-methylated at K20. **b,** HeLa cells transfected with either control or *SMC4* siRNAs were lysed 72 h after transfection and subjected to immunoblotting analysis as indicated. **c,** Validation of SMC4 binding sites in M phase HeLa cells revealed by ChIP-Seq. Cells transfected with siRNAs as described in (b) were subjected to standard ChIP-qPCR analysis. ChIP signals were presented as % of Inputs (± s.e.m.). ChIP signals for all 36 selected putative SMC4 binding sites showed enrichment over a negative control region and decreased after knock-down of SMC4.

Sample	Total Reads	Aligned Reads (uniquely aligned reads & the reads that align to repetitive regions)	Uniquely Aligned Reads
PHF8 (unsynchronized)	37,439,557	12,429,834	9,768,104
PHF8 (G1 phase)	20,037,406	11,782,825	9,584,043
PHF8 (S phase)	31,939,089	14,944,104	11,845,100
H3K4me^2 (unsynchronized)	2,029,718	1,566,645	1,240,010
E2F1 (unsynchronized)	16,367,661	7,785,017	7,339,848
H4K20me^1 (M phase)	16,361,110	12,923,394	9,263,695
SMC4 (M phase)	13,437,787	7,224,333	5,261,263

Figure S18, Summary of ChIP-Seq reads for PHF8, H3K4me^2, E2F1, H4K20me^1 and SMC4.